ORIGINAL ARTICLE

Small Molecule Rescue of ATXN3 Toxicity in *C. elegans* via TFEB/HLH-30

Yasmin Fardghassemi [1,2] · Claudia Maios [1,3] · J. Alex Parker [1,2,3]

Abstract

Spinocerebellar ataxia type 3 (SCA3), also known as Machado-Joseph disease (MJD), is a polyglutamine expansion disease arising from a trinucleotide CAG repeat expansion in exon 10 of the gene *ATXN3*. There are no effective pharmacological treatments for MJD, thus the identification of new pathogenic mechanisms, and the development of novel therapeutics is urgently needed. In this study, we performed a comprehensive, blind drug screen of 3942 compounds (many FDA approved) and identified small molecules that rescued the motor-deficient phenotype in transgenic *ATXN3 Caenorhabditis elegans* strain. Out of this screen, five lead compounds restoring motility, protecting against neurodegeneration, and increasing the lifespan in *ATXN3*-CAG89 mutant worms were identified. These compounds were alfacalcidol, chenodiol, cyclophosphamide, fenbufen, and sulfaphenazole. We then investigated how these molecules might exert their neuroprotective properties. We found that three of these compounds, chenodiol, fenbufen, and sulfaphenazole, act as modulators for TFEB/HLH-30, a key transcriptional regulator of the autophagy process, and require this gene for their neuroprotective activities. These genetic-chemical approaches, using genetic *C. elegans* models for MJD and the screening, are promising tools to understand the mechanisms and pathways causing neurodegeneration, leading to MJD. Positively acting compounds may be promising candidates for investigation in mammalian models of MJD and preclinical applications in the treatment of this disease.

Key Words Machado-Joseph disease · neurodegenerative diseases · *Caenorhabditis elegans* · ataxin-3 · drug screening · neuroprotective compounds · TFEB/HLH-30.

Abbreviations

MJD	Machado-Joseph disease
SCA	Spinocerebellar ataxia
SCA3	Spinocerebellar ataxia type 3
PD	Parkinson's disease
AD	Alzheimer's disease
ALS	Amyotrophic lateral sclerosis
ATXN3	Ataxin-3
TFEB	Transcription factor EB
HLH-30	Helix-loop-helix 30
FDA	Food and Drug Administration

✉ J. Alex Parker
ja.parker@umontreal.ca

Yasmin Fardghassemi
yasmin.fard.ghassemi@umontreal.ca

Claudia Maios
claudiamaios@gmail.com

1 Centre de Recherche du Centre Hospitalier de l'Université de Montréal (CRCHUM), Montreal, Quebec H2X 0A9, Canada

2 Department of Biochemistry, University of Montreal, Montreal, Quebec H3T 1J4, Canada

3 Department of Neuroscience, University of Montreal, Montreal, Quebec H3T 1J4, Canada

Introduction

SCA3 (spinocerebellar ataxia type 3), also known as Machado-Joseph disease (MJD), is considered to be the most common form of SCA worldwide [1]. SCAs are considered to be rare disorders, with a prevalence ranging from 0.3 to 2.0 per 100,000 [2]. MJD, a polyglutamine expansion disease, is a hereditary autosomal dominant neurodegenerative disease that develops when there is an abnormal expansion of the trinucleotide cytosine-adenine-guanine (CAG) repeats in the causative gene [3–5]. MJD is characterized mainly by ataxia, spasticity, peripheral muscular atrophy, and/or other motor-related clinical manifestations along with neurodegeneration

in selective regions including the cerebellum, basal ganglia, brainstem, and spinal cord [5–8]. MJD is more highly observed among people of Portuguese/Azorean with the highest prevalence in the Azorean island of Flores (1/239) [9]. This disease is caused by an unstable expansion of CAG trinucleotide within the coding region of *ATXN3* gene, located on chromosome 14 (14q24.3-14q32.45) [3, 10–12]. The CAG repeat number in healthy individuals is between 10 and 51, whereas in SCA3 patients, this repeat is expanded to 55–87 [13, 14]. The mutated *ATXN3* gene is translated into an abnormal polyglutamine (poly-Q) tract within the ataxin-3 protein (ATXN3) [10, 15]. The abnormal expansion in the *ATXN3* gene leads to misfolding of ATXN3 and is associated with numerous harmful impacts such as generation of toxic poly-Q protein species, protein aggregation, disrupted protein homeostasis, loss of deubiquitylase activity, and dysregulation of autophagy, among others [3, 16]. However, the exact mechanisms of disease pathogenesis, as well as molecular pathways, are still not well understood. This restraint knowledge prevents the development of possible clinical therapies to cure or even attenuate the phenotypes associated with this disease.

To investigate aspects of MJD, we turned to the simple animal model, *Caenorhabditis elegans*, a popular system for neuroscience investigations [17]. *C. elegans* is especially well-suited for neuroscience and genetic research due to the large number of conserved molecular pathways resembling that of vertebrates and its ease of genetic manipulation [18, 19]. Furthermore, *C. elegans* has been used to model several neurodegenerative diseases such as MJD, amyotrophic lateral sclerosis (ALS), Parkinson's disease (PD), and Alzheimer's disease (AD) [6, 20–26].

C. elegans is also a useful system for drug discovery and linking drug activity to specific genetic and molecular pathways required for action. It is a powerful tool for the therapeutic discovery of compounds that are able to restore the disease phenotype, such as motility, and also to identify specific molecular pathways [27, 28]. We have previously shown that our transgenic *ATXN3* mutant worms display motility defects, along with progressive neurodegeneration and reduced longevity [20]. Based on these findings, the goal of this study was to identify small molecules with neuroprotective effects that could be translated along preclinical and clinical pathways for MJD. To achieve this goal, we conducted a blind drug screen of 3942 compounds and identified lead compounds that suppressed motor deficits of *ATXN3* mutant worms, and rescued accompanying neurodegeneration and reduced longevity phenotypes. Among the lead compounds, chenodiol, fenbufen, and sulfaphenazole rescued the *ATXN3* toxicity by acting as modulators of the transcription factor EB (TFEB/HLH-30), a transcription factor implicated in autophagy. These molecules are promising tools to improve neuronal health and survival in MJD models, warranting investigation in vertebrate systems.

Materials and Methods

Nematode Strains and Maintenance

Standard methods of culturing and handling worms were used [19]. Worms were maintained on standard nematode growth media (NGM) plates streaked with OP50 *E. coli*. All strains were scored at 20 °C. Strains used for this study were N2, MAH240 *sqIs17*[*hlh-30*p::*hlh-30*::GFP + *rol-6(su1006)*] and *hlh-30(tm1978)*, all obtained from the *Caenorhabditis* Genetics Center (University of Minnesota, Minneapolis).

Transgenic *ATXN3* Worms and Plasmid Constructs

The development of our transgenic *ATXN3* worms is explained in our previous paper [20]. The strain used in this study include: XQ351 *unc-119(ed3)*; ttTi5605mosII; *xqIs351*(*unc-47*p::*ATXN3*-CAG89; *unc-119(+)*), referred to as *ATXN3*-CAG89. As previously shown, these transgenic mutants have motility defects, neurodegeneration, and reduced longevity.

Drug Libraries

The Sigma LOPAC library, composed of 1280 bioactive compounds; the MicroSource Discovery library, containing 880 compounds; the Biomol Natural Products library (Enzo Life Sciences, Inc.), composed of 500 compounds; and the Prestwick Chemical library, containing 1282 compounds, were selected for the worm-based motility screenings. All compounds were dissolved in DMSO (dimethyl sulfoxide) and tested at a concentration of 20 μM for 4 h.

Drug Screen

The drug screen was performed by using a WMicroTracker machine (Phylum Tech) [29]. Briefly, ~ 50–60 worms adult day one were exposed to the drugs at a concentration of 20 μM, or to DMSO as the control in a 96-well plate. The swimming movement was tracked for at least 4 h. Measurements were performed in triplicates and the average movement score was compared to the control and the average movement score of the whole plate. If the values were higher than the respective controls for a certain drug, then a secondary screen was performed to validate our observations. Candidates that increased significantly the swimming movement in the secondary screen were considered as positive hits.

Age-Synchronized Populations

To obtain age-synchronized worms, ~ 10 adult hermaphrodites were placed on ten NGM plates for 3–4 days and kept at 20 °C. Once the plates were full of adult worms, they were

collected with M9 buffer (1 M KH_2PO_4, 1 M Na_2HPO_4, 1 M NaCl, 1 M $MgSO_4$) and centrifuged at 4000 rpm (A-4-81 Rotor) for 2 min at 4 °C. After centrifugation, 3 mL of the supernatant was taken and replaced with 3 mL of a mix solution containing NaOH 5 M and bleach (1:2). A 5-min vortex followed with a high intensity to degrade the worms leaving a pellet containing only eggs. The pellet was washed 3 times with M9 buffer and centrifuged at 4000 rpm (A-4-81 Rotor) for 2 min at 4 °C. The pellet was transferred onto NGM plates without bacteria and kept overnight at 20 °C. The following day, L1 worms were transferred using M9 buffer onto plates streaked with OP50 *E. coli* and are kept at 20 °C.

Paralysis Assays on Solid Media

Worms were scored for paralysis from adult day one to adult day twelve. Thirty L4 worms were transferred to NGM plates. They were scored as paralyzed if they failed to move after being prodded with a worm pick. Worms were scored as dead if they were unable to respond to tactile head stimulus. All experiments were conducted at 20 °C, and each condition was done in triplicate with 30 worms/plate.

Lifespan Assays

Forty L4 worms were transferred to NGM plates and tested every 2 days from adult day one until death. They were scored as dead if they failed to respond to tactile stimulus and showed no spontaneous movement or response when prodded. Dead worms displaying internally hatched progeny, extruded gonads, or that crawled off the plate were excluded. All experiments were conducted at 20 °C, and each condition was done in triplicates with 40 worms/plate.

Fluorescence Microscopy (Neurodegeneration and Stress Reporter Fluorescence Quantification)

For scoring of neuronal processes for gaps or breakages, worms were collected at adult day five and day nine for visualization of motor neuron processes in vivo. For fluorescence quantification of the stress reporter, *hlh-30*::GFP, *hlh-30*::GFP; *ATXN3*-CAG10 and *hlh-30*::GFP; *ATXN3*-CAG89 worms were collected at adult day one, two, three, and five. The nematodes were immobilized with 60% glycerol and mounted on slides with 2% agarose pads. mCherry was visualized at 595 nm and GFP was visualized at 488 nm using a Zeiss Axio Imager M2 microscope. Fluorescent expression was visualized with a DIC microscope Zeiss AxioObserver A1. The software used was AxioVs40 4.8.2.0. One hundred to one hundred fifty worms were scored per condition for the neurodegeneration assays. Approximately 17 to 20 worms were visualized per condition for the fluorescence quantification experiments. Image processing and quantification were done with Adobe Photoshop. For the fluorescence quantification of the stress reporter, we calculated the changes in the ratio (size/intensity of fluorescence). One-way ANOVA test was used for statistical analysis.

Compound Treatment on Solid Media

Worms were exposed from L4 state to compounds at 20 μM or 2 μM (with 1% DMSO or 0.1% DMSO final concentration, respectively) incorporated into an NGM solid medium, or an NGM solid medium only as a control. All the plates were streaked with OP50 *E. coli.* The five lead compounds were purchased from Sigma-Aldrich (St. Louis, MO), Cayman Chemical Co. (Ann Arbor, MI), or Toronto Research Chemicals Inc. (North York, TO). Briefly, 30–40 worms were picked and plated on the corresponding NGM medium (30–40 worms/plate for each condition and each condition was done in triplicate) in order to complete the paralysis and lifespan assays, the neurodegeneration observations, and fluorescence quantification (fluorescence microscopy).

Cheminformatics

Each pair of compounds to be analyzed for similarity was evaluated for the presence or absence of any of thousands of possible FP2 fingerprints. The Tanimoto coefficient also known as the Jaccard index represents one of the most popular methods for quantifying molecular similarity. Tanimoto coefficient scores were calculated for each hit and compound present in the Prestwick library using OpenBabel (http://openbabel.org) [30, 31].

To enhance the effectiveness of similarity of molecules, Tanimoto scores higher than 0.50 were clustered using an unweighted Euclidean distance similarity metric with complete linkage clustering allowing visualization of the ranked molecules within the context of the dendrogram. Enrichment for the structural similarity of members in each cluster (Tanimoto scores were > 0.50 for majority of members in a cluster) was calculated using Fisher's exact test (GraphPad Prism Software) [31].

The heat maps were generated using: https://software.broadinstitute.org/morpheus/. This tool uses R software (R Team: R Development Core Team (2005). R: A language and environment for statistical computing. R Foundation for Statistical Computing, Vienna, Austria. ISBN 3-900051-07-0, www.R-project.org.).

Statistics

Paralysis and lifespan curves were generated and compared using the log-rank (Mantel-Cox) test. For neurodegeneration and the fluorescence assays, one-way ANOVA tests were used. All experiments were repeated at least three times. For

the heat map statistics, Fisher's exact tests were realized. Prism (GraphPad Software) was used for all statistical analyses.

Results

Chemical-Genetic Screen in *ATXN3* Mutant *C. elegans*

Our previous work demonstrated that the motility defects observed in *ATXN3*-CAG89 transgenic worms could be rescued using specific small molecules [20]. This promising prescreen encouraged us to go further, so we performed a blind, liquid culture, drug screen of 3942 small molecules (at 20 μM) for the rescue of motility defects in *ATXN3*-CAG89 transgenic

worms, and identified 24 lead molecules (Fig. 1, Supplementary Table S1, Supplementary Table S2).

To validate these findings, the *ATXN3*-CAG89 mutant worms were then treated with the positive compounds using a solid media approach (Fig. 2A–C), and 21 of the initial 24 compounds maintained rescuing activity (clebopride, lamotrigine, and phorbol 12-myristate 13-acetate were rejected) (Fig. 2A–C). These differences could be due to the acute nature of the liquid drug screen where the animals are exposed to molecules over a period of 4 h, compared to drug exposure over 12 days using solid media assays.

The compounds were then tested at a lower dose (2 μM) and we observed that 13 of the 21 compounds showed significant suppression of the locomotion deficit in *ATXN3*-CAG89 transgenics at this concentration (Fig. 3A, B). We further
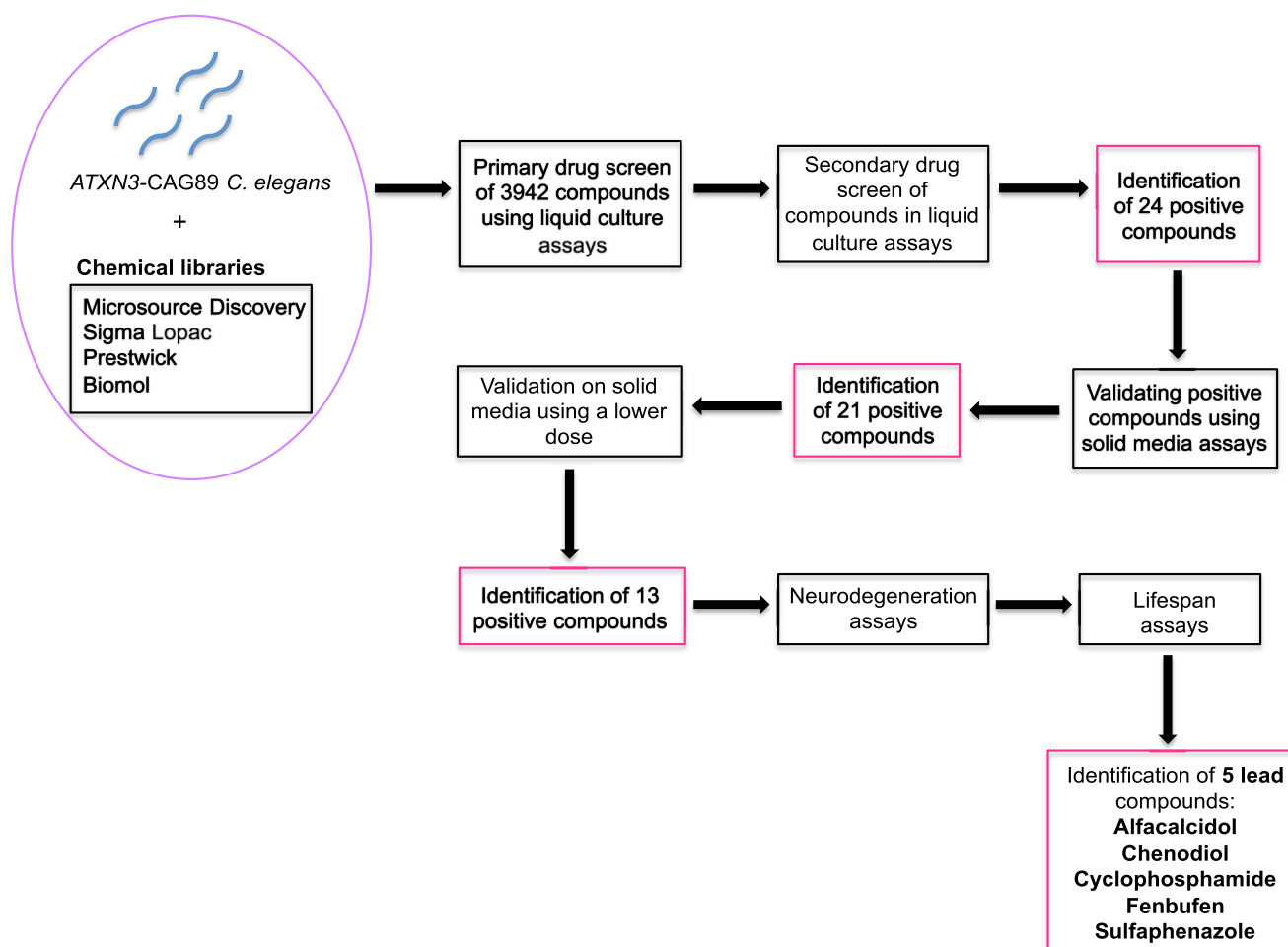

Fig. 1 Chemical-genetic screen in *ATXN3*-CAG89 mutant transgenics. By using the *WMicroTracker* machine, 3942 compounds with 20 μM concentration were screened in our MJD strain. These compounds were, from four companies: Microsource Discovery, Sigma Lopac, Prestwick, and Biomol. Measurements were performed in triplicates and the average movement score was compared to the control (*ATXN3*-CAG89 mutants in DMSO, no compound) and the average movement score of the whole plate. If the values were higher than the respective controls for a certain drug, then a secondary screen was performed to validate our observations. Candidates that increased significantly the swimming movement in the secondary screen were considered as positive hits. From this screen, we identified 24 positive compounds able to significantly correct the impaired movement phenotype of our MJD strain when compared to the controls. After paralysis, neurodegeneration, and lifespan assays, we identified five lead compounds able to rescue all these phenotypes. The lead compounds are: alfacalcidol (ALFA), chenodiol (CHEN), cyclophosphamide (CYCLO), fenbufen (FEN), and sulfaphenazole (SULFA)
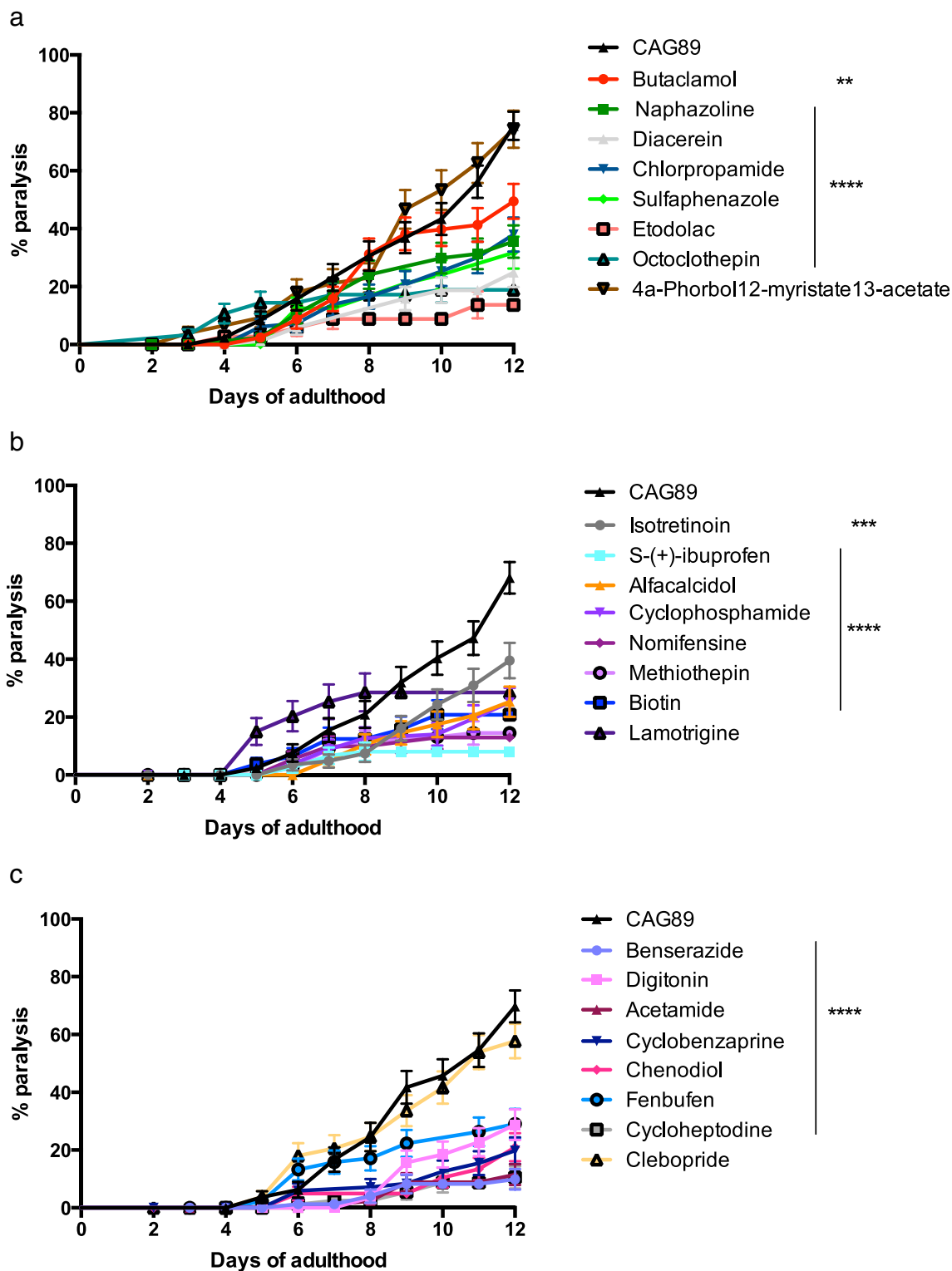
Fig. 2 Validation of the positive compounds on solid media assays. (**a**–**c**) The motor defect phenotype observed in *ATXN3*-CAG89 worms was significantly rescued when treated with (**a**) butaclamol (**$**P < 0.01$), or naphazoline, diacerein, chlorpropamide, sulfaphenazole, etodolac, octoclothepin (****$P < 0.0001$ for all previous compounds); (**b**) isotretinoin (***$P < 0.001$), ibuprofen, alfacalcidol, cylclophosphamide, nomifensine, methiothepin, biotin (****$P < 0.0001$ for all mentioned compounds); (**c**) benserazide, digitonin, acetamide, cyclobenzaprine, chenodiol, fenbufen, and cycloheptadine (****$P < 0.0001$ for all previous compounds) (by log-rank (Mantel-Cox) test, $N = 90–100$ per trial, and $N = 270–300$ when all trials combined). No rescue of the locomotion defect is observed when the *ATXN3*-CAG89 worms were treated with phorbol 12-myristate 12-acetate, lamotrigine, or clebopride. The concentration of the compounds was tested at 20 μM as in the liquid culture. This experiment was done 3 times

tested these 13 compounds at two additional concentrations (0.2 μM and 40 μM), and we conclude that the optimal concentration for these compounds to suppress the paralysis phenotype in our MJD model, among the ones that have been evaluated for this study, is set at 2 μM.

Small Molecules Rescue the Neurodegeneration and Extend Lifespan in *ATXN3*-CAG89 Transgenics

ATXN3-CAG89 transgenics display progressive degeneration of motor neurons as they age [20], and we focused on days five and nine of adulthood to evaluate the neuroprotective capacity of the 13 lead compounds. The health of motor neurons in *ATXN3*-CAG89 transgenics was assessed with a stably integrated *unc-47*p::mCherry translated that expresses a red fluorescing protein in the GABAergic motor neurons of living animals. Using this *ATXN3*-CAG89; *unc-47*p::mCherry strain, we observed that seven compounds rescued neurodegeneration at day five of adulthood (Fig. 3C). These seven compounds were then tested on *ATXN3*-CAG89 mutant worms and neurodegeneration was examined at adult day nine, and significant rescue of neurodegeneration was observed when treated with the following five compounds: alfacalcidol (ALFA), chenodiol (CHEN), cyclophosphamide (CYCLO), fenbufen (FEN), and sulfaphenazole (SULFA) (Fig. 3D). Finally, these five compounds rescued the decreased lifespan phenotype observed in *ATXN3*-CAG89 transgenics (Fig. 3E). Altogether, we identified five molecules that suppressed several negative phenotypes associated with the expression of mutant ATXN3 in vivo.

Heat Map Visualization of the Five Hit Compounds and Their Chemical Classes

Afterward, we wondered to evaluate the structural similarity and similar clusters existing between either the hit or not hit compounds screened from the 1280 molecules present in the Prestwick library (all five identified leads in this study belong to this library). From the hit compounds, several chemical classes were more representative: vitamin D3 derivatives (**$P = 0.0078$), cyclophosphamides (**$P = 0.0078$), benzenes (*$P = 0.0233$), and sulfonamides (*$P = 0.0271$) in which belong ALFA, CYCLO, FEN, and SULFA, respectively (Suppl. Fig. 1, Supplementary Material). All these chemical classes were statistically overrepresented, except the steroids (ns; $P = 0.0610$), CHEN, which strongly suppressed the phenotypes but were not statistically overrepresented (Suppl. Fig. 1, Supplementary Material). This could be due to the fact that more compounds were represented in this category (16 compounds) compared to the others, and also, a high structural similarity was observed between different isoforms in this chemical class.

Involvement of TFEB/HLH-30, a Key Regulator of the Autophagy Process in MJD

Autophagy is a major cellular recycling pathway that has an important role in aging. Several studies have highlighted an important link between autophagy and neurodegenerative diseases, and disruption of this pathway may contribute to pathology [3, 32, 33]. It has also been shown that upregulation of this pathway could be beneficial and ameliorate disease pathology [32]. Transcription factor EB (TFEB) is a major regulator of autophagy and lysosomal gene expression, and *C. elegans* possesses an orthologue named HLH-30 [34]. Based on this, we wondered if upregulation of TFEB/HLH-30 could modify phenotypes in our *C. elegans* MJD model. We crossed our *ATXN3* transgenics with a transgenic,

Fig. 3 Rescue of motility deficit, neurodegeneration and reduce ▶ longevity when *ATXN3*-CAG89 worms are treated with positive compounds at 2 μM. (A–B) Mutant transgenic worms showed a rescue of locomotion impairment when treated with 2 μM (**a**) cyclophosphamide, methiotepin, diacerein, alfacalcidol, butaclamol, sulfaphenazole, chenodiol, fenbufen, or nomifensin (****$P < 0.0001$ for all the compounds), as well as (**b**) naphazoline (*$P < 0.05$), benserazide (**$P < 0.01$), acetamide or chlorpropamide (*$P < 0.05$ for both compounds) (by log-rank (Mantel-Cox) test, $N = 90–100$ per trial, and $N = 270–300$ when all trials combined). This experiment was replicated 3 times. (**c–d**) Shown are representative photos of living, adult expressing *unc-47*p::mCherry; *ATXN3*-CAG89 transgenic worms at day five and day nine of adulthood with or without drug. The concentration of drugs used for this experience is 2 μM. Images are black and white. Arrows indicate gaps or breaks along neuronal processes. (**c**) Images of the GABAergic motor neurons from an entire *unc-47*p::mCherry; *ATXN3*-CAG89 transgenic worms at adulthood day five with or without drug. Quantification of neurodegeneration in *unc-47*p::mCherry; *ATXN3*-CAG89 worms at day five of adulthood. Significant neurodegeneration is observed in *unc-47*p::mCherry; *ATXN3*-CAG89 transgenics when compared to the control, *unc-47*p::mCherry (####$P < 0.0001$). Significant rescue of the neurodegeneration morphology was observed in *unc-47*p::mCherry; *ATXN3*-CAG89 worms when treated with 2 μM diacerein (**$P < 0.01$), butaclamol, fenbufen, chenodiol, alfacalcidol, sulfaphenazole or cyclophosphamide (****$P < 0.0001$ for all the previous compounds) (by one-way ANOVA test, $N = 150$ for each condition). These experiments were done 6 independent times ($N = 25$ per trial for each condition). (**d**) Images of degenerating GABAergic motor neurons of *unc-47*p::mCherry; *ATXN3*-CAG89 transgenic worms at adulthood day nine with or without drug. Quantification of neurodegeneration in transgenic *unc-47*p::mCherry; *ATXN3*-CAG89 worms at day nine of adulthood. Significant neurodegeneration is observed in *unc-47*p::mCherry; *ATXN3*-CAG89 transgenics when compared to the control, *unc-47*p::mCherry (####$P < 0.0001$). This neurodegeneration is rescued when *unc-47*p::mCherry; *ATXN3*-CAG89 worms are treated with fenbufen, chenodiol, alfacalcidol, sulfaphenazole, or cyclophosphamide (****$P < 0.0001$ for all compounds) (by one-way ANOVA test, $N = 150$ for each condition). These experiments were repeated 6 times ($N = 25$ per trial for each condition). (**e**) Increased lifespan in *ATXN3*-CAG89 worms when treated with 2 μM CYCLO, ALFA, FEN, or SULFA (****$P < 0.0001$ for all four compounds), or CHEN (**$P < 0.01$) (by log-rank (Mantel-Cox) test) ($N = 300–360$). The experiment was done 3 times
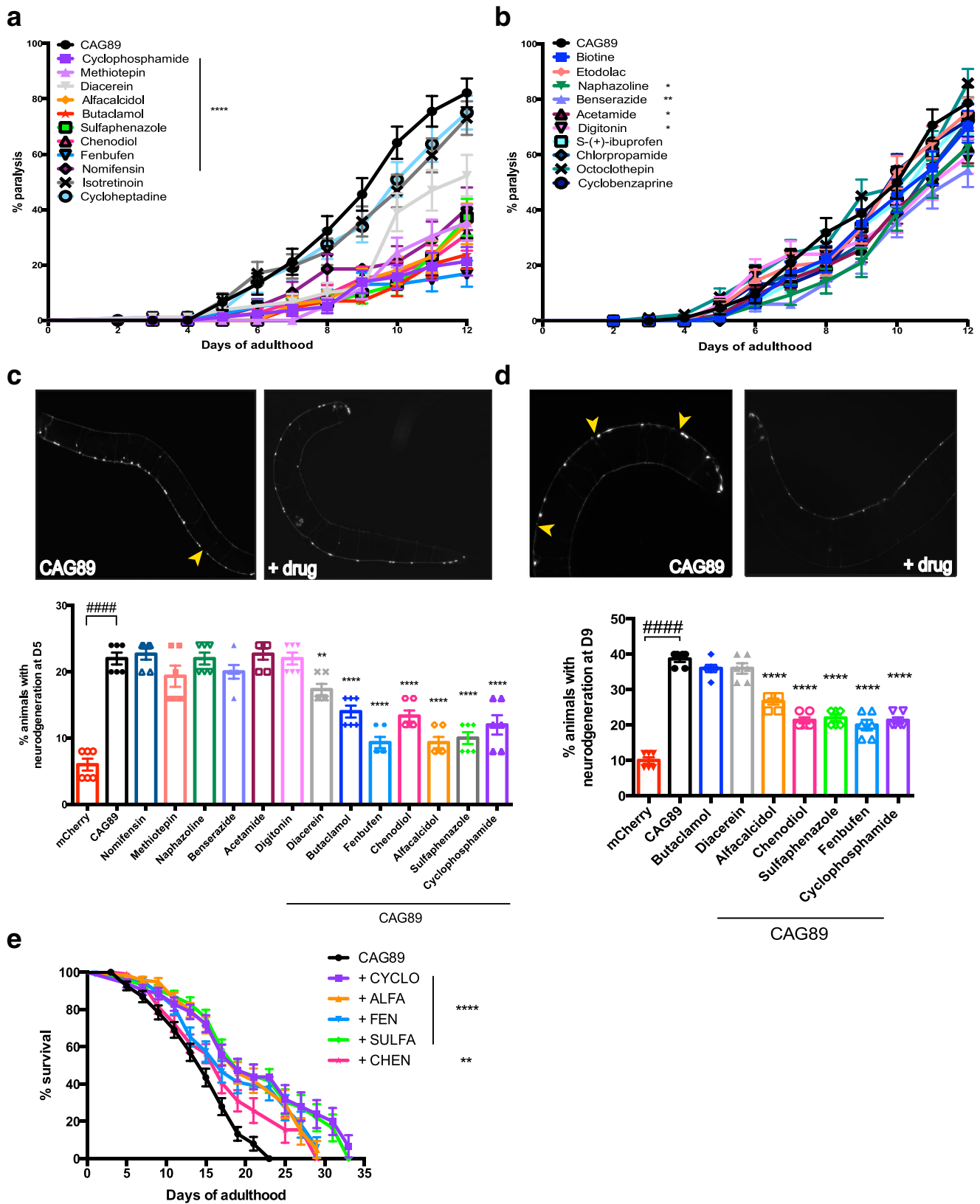
translational *hlh-30* reporter strain which uses the *hlh-30* promoter to express *hlh-30* fused to GFP and measured the level of fluorescence in different adulthood stages: day one, two, three and five. No difference in the level of fluorescence was

observed in day one of adulthood between treated or untreated *hlh-30*::GFP, *hlh-30*::GFP; *ATXN3*-CAG10 and *hlh-30*::GFP; *ATXN3*-CAG89 transgenic worms. However, we observed increased fluorescence in *hlh-30*::GFP; *ATXN3*-CAG89 worms when compared to *hlh-30*::GFP or *hlh-30*::GFP; *ATXN3*-CAG10 controls at adulthood days two, three, and five (Fig. 4A, B, Suppl. Fig. 2). This increase of fluorescence was mostly observed in the head (H), spermatheca (S), and tail (T). These data suggest there is an upregulation of the autophagy process in response to toxicity induced by mutant poly-Q proteins. From here, we investigated the activity of the lead compounds in relation to *hlh-30* expression. We found that three out of the five compounds (exceptions were ALFA and CYCLO) decreased the fluorescence level in *ATXN3*-CAG89 mutant worms at adulthood days two and three (Suppl. Fig. 2), but significantly increased it at adulthood day five (Fig. 4A, B). We observed that in aging worms, *hlh-30*::GFP expression tends to shift and increase in *ATXN3*-CAG89 transgenics when treated with CHEN, FEN, and SULFA. We observed that the decreased level of fluorescence related to *hlh-30*::GFP expression in treated *ATXN3*-CAG89 worms at adulthood day three is less severe than adulthood day two, and increased at adulthood day five in the treated worms. This suggests that the increased expression of HLH-30 in *ATXN3*-CAG89 worms may represent an autophagic stress response that is mitigated by the small molecules CHEN, FEN, and SULFA in the early stages of worms (adulthood day two and three) but with aging, in a longer-term matter (adulthood day five), the molecules increase the level of HLH-30 expression in our MJD worms in order to protect the organism and decrease the toxicity caused by mutant ATXN3. We observed no effect of the compounds in *hlh-30*::GFP or *hlh-30*::GFP; *ATXN3*-CAG10 worms at different stages when treated (Suppl. Fig. 2). These data suggest a possible link between mutant ATXN3 toxicity and autophagy, as detected via *hlh-30* expression. Although, further experiments would be required in order to be able to answer if the link existing between the action of the compounds and the autophagy in MJD mutants is due to a direct or indirect effect involving additional mechanisms and pathways.

Chemical-Genetic Modulation of *hlh*-30 Suppresses the Neuronal Toxicity Observed in *ATXN3*-CAG89 Worms

Next, we examined directly for neuroprotective effects of increased *hlh-30* expression in conjunction with the five lead molecules. We observed a decreased rate of paralysis in *hlh-30*::GFP; *ATXN3*-CAG89 worms when compared to *ATXN3*-CAG89 controls (Fig. 5A). Indeed, overexpression of HLH-30 alleviates the motility defect observed in *ATXN3*-CAG89 mutant worms. We tested the five lead molecules in the *hlh-30*::GFP; *ATXN3*-CAG89 worms, and although they all suppressed paralysis (Fig. 5A) and motor

neuron degeneration (Fig. 5B) compared to *ATXN3*-CAG89 controls, only FEN showed an additive effect compared to *hlh-30*::GFP; *ATXN3*-CAG89 controls. These data suggest that upregulation of HLH-30 and treatment of the MJD model with FEN could be a novel neuroprotective approach to undertake in order to decrease the neuronal toxicity caused by expanded ATXN3.

CHEN, FEN, and SULFA Require *hlh-30* for Their Neuroprotective Activities

To determine if any of the five lead molecules required *hlh-30* for their neuroprotective activity, and in order to confirm if the link existing between *hlh-30* and the action of the compounds is due to a direct or indirect effect, *ATXN3*-CAG89 worms were crossed with loss-of-function (LOF) mutant *hlh-30* worms. We observed that CHEN, FEN, and SULFA required *hlh-30* for their activity as these compounds were unable to rescue motility deficits (Fig. 6A) and neurodegeneration (Fig. 6B) in *hlh-30(tm1978)*; *ATXN3*-CAG89 worms. Treatment with CYCLO or ALFA continued to rescue paralysis and neurodegeneration phenotypes in the absence of *hlh-30* (Fig. 6), suggesting a possible compensatory effect by other pathways. Also, we observed in the paralysis assays that *hlh-30(tm1978)*; *ATXN3*-CAG89 worms showed a slightly lower (but not significant) paralysis phenotype when compared to *ATXN3*-CAG89 mutants, suggesting a possible rescue effect in our MJD model when *hlh-30* is absent (Fig. 6A). However, with the neurodegeneration assays, this hypothesis was rejected as we observed a slight increase (without showing significance) of neurodegeneration in *hlh-30(tm1978)*; *ATXN3*-CAG89 worms compared to *ATXN3*-CAG89 mutants (Fig. 6B). These data show that the absence of *hlh-30* in our MJD model does not necessarily modify *ATXN3*-CAG89

Fig. 4 Involvement of TFEB/HLH-30, a key regulator of the autophagy ▶ process in MJD. (**a**) Shown are representative photos of living, adult *hlh-30::*GFP, *hlh-30*::GFP; *ATXN3*-CAG10 and *hlh-30*::GFP; *ATXN3*-CAG89 transgenics at day five of adulthood. *hlh-30*::GFP; *ATXN3*-CAG89 transgenics showed increase GFP expression compared to *hlh-30*::GFP, or *hlh-30*::GFP; *ATXN3*-CAG10 controls (top panels). Treatment with 20 μM CHEN, 20 μM FEN, or 20 μM SULFA increased fluorescence of *hlh-30*::GFP; *ATXN3*-CAG89 mutants. *hlh-30*::GFP reporter showed increase fluorescence in the head (H), spermatheca (S), and tail (T) of adult animals. (**b**) Quantification of fluorescence of transgenics with or without treatment with compounds. An increased fluorescent signal was observed in *hlh-30*::GFP; *ATXN3*-CAG89 worms compared to *hlh-30*::GFP or *hlh-30*::GFP; *ATXN3*-CAG10 controls ($^{###}P < 0.001$ and $^{#}P < 0.05$ respectively). A significantly increased fluorescence was observed in *hlh-30*::GFP; *ATXN3*-CAG89 mutants when treated with 20 μM CHEN ($^*P < 0.05$), 20 μM FEN ($^{**}P < 0.01$) or 20 μM SULFA ($^*P < 0.05$) (by one-way ANOVA test, $N = 17$–20 per trial for each condition). We observed no change in the fluorescence when *hlh-30*::GFP; *ATXN3*-CAG89 mutants were treated with 20 μM CYCLO or 20 μM ALFA. These experiments were replicated 3 times

phenotypes, but confirm that CHEN, FEN, and SULFA require *hlh-30* for their neuroprotective activities, as well as a direct link between *hlh-30* and the action of these three compounds.
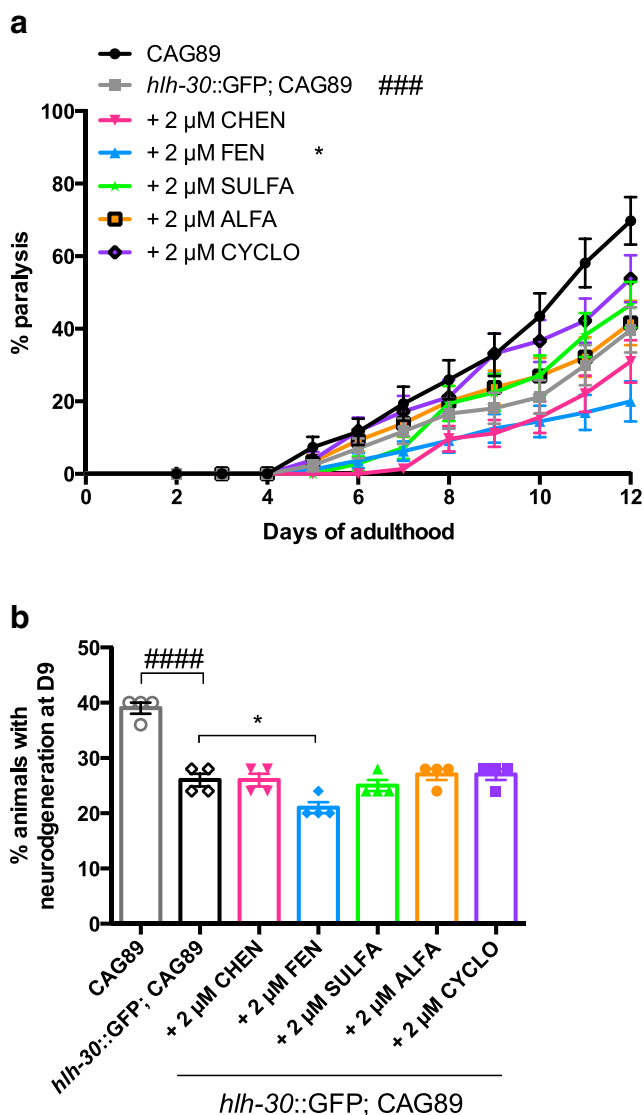
a

b
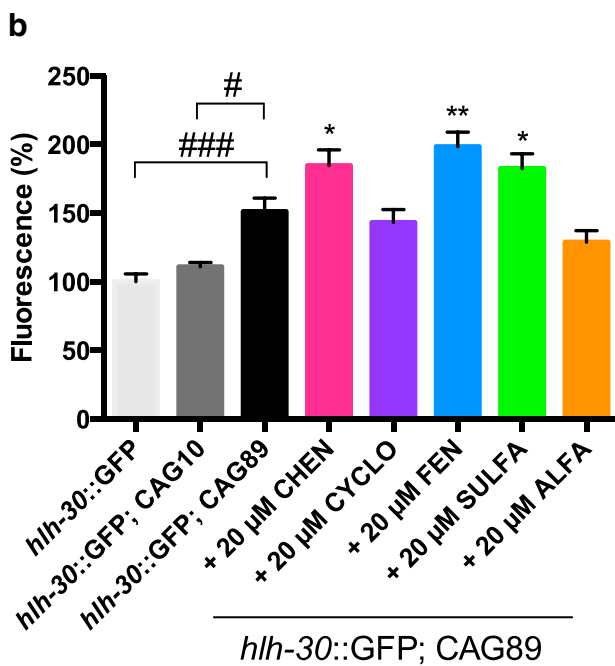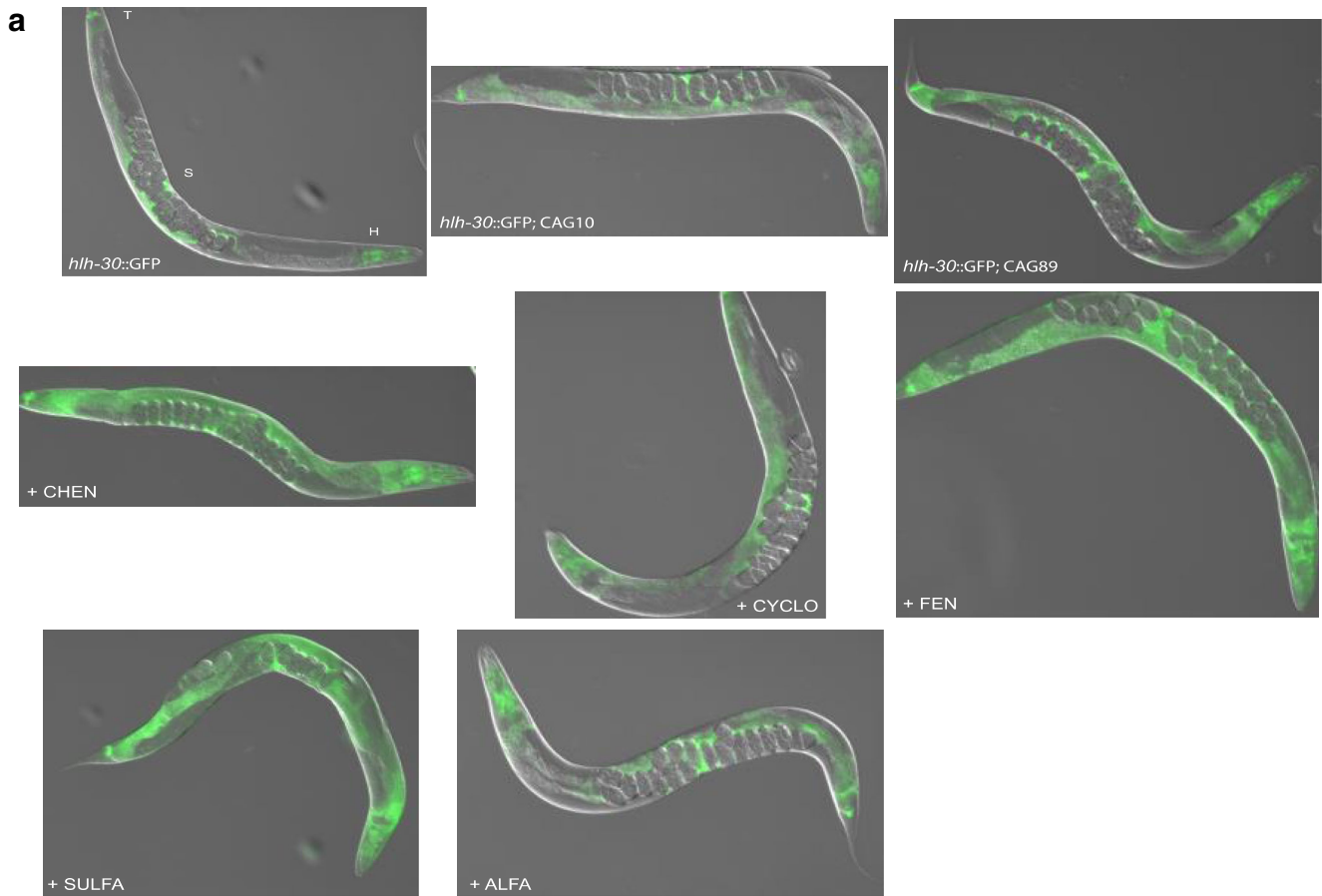
Fig. 5 Chemical-genetic modulation of *hlh-30* suppresses the neuronal toxicity observed in *ATXN3*-CAG89 worms. (**a**) Decreased motility defect in *hlh-30*::GFP; *ATXN3*-CAG89 worms when compared to the control, *ATXN3*-CAG89 transgenics ($^{###}P < 0.001$). When *hlh-30*::GFP; *ATXN3*-CAG89 worms are treated with 2 μM CHEN, 2 μM ALFA, 2 μM SULFA, or 2 μM CYCLO a similar profile to non-treated worms is observed. Rather, a significant rescue of motility is observed in *hlh-30*::GFP; *ATXN3*-CAG89 when treated with 2 μM FEN ($^*P < 0.05$) (by log-rank (Mantel-Cox) test, $N = 90–100$ per trial, and $N = 270–300$ when all trials combined). These experiments were replicated 3 times. (**b**) Quantification of neurodegeneration in *hlh-30*::GFP; (*unc-47*p::mCherry; *ATXN3*-CAG89) worms at day nine of adulthood. Significant rescue of neurodegeneration in *hlh-30*::GFP; (*unc-47*p::mCherry; *ATXN3*-CAG89) worms was observed when compared to the control at adulthood day nine ($^{####}P < 0.0001$). Treatment of the worms with 2 μM CHEN, 2 μM ALFA, 2 μM SULFA, or 2 μM CYCLO showed no additional rescue when compared to untreated *hlh-30*::GFP; (*unc-47*p::mCherry; *ATXN3*-CAG89) worms. Treatment of *hlh-30*::GFP; (*unc-47*p::mCherry; *ATXN3*-CAG89) worms with 2 μM FEN ($^*P < 0.05$) (by one-way ANOVA test, $N = 100$ for each condition) showed a significant rescue of the neurodegeneration profile. These experiments were done 4 times

Finally, we tested treatment with the three compounds (CHEN, FEN, and SULFA) and observed that they failed to suppress motility phenotypes in *hlh-30(tm1978); ATXN3*-CAG89 worms (Fig. 7A), whereas the triple molecule treatment provided robust suppression in *hlh-30*::GFP; *ATXN3*-CAG89 worms (Fig. 7B). These results demonstrate a key role for *hlh-30* in the suppression of mutant ATXN3 toxicity by small molecules.

Discussion

By using our *ATXN3* transgenic worms, we performed a large comprehensive blind drug screen of 3942 molecules. This screen allowed us to identify five lead compounds that rescued the motor function, neurodegeneration, and reduced longevity observed in our *ATXN3* mutant transgenic *C. elegans*. Besides finding five lead compounds, we also identified a new transcription factor related to *ATXN3* toxicity, TFEB/HLH-30. We also showed that chenodiol, fenbufen, and sulfaphenazole, are dependent on this transcription factor for their neuroprotective activities in MJD.

Drug screening in *C. elegans*, a simple and easily maintained model organism, is a popular tool to identify compounds, as well as pathways contributing to a better understanding of the disease and development of possible therapies [18, 35–37]. In this study, we used this approach in order to find lead molecules able to rescue the locomotion deficit observed in our mutant *ATXN3*-CAG89 transgenics. The aim of this study was to identify molecules and pathways related to MJD, as well as potential compounds for drug development in the treatment of MJD. The drug library we screened contained many FDA-approved compounds allowing for rapid, potential translation to preclinical settings. Also, many of the compounds in this library have been studied and tested in models for other neuropathologies such as Alzheimer's disease, Parkinson's disease, and ALS. The screening and other assays (paralysis, neurodegeneration, and lifespan) allowed us to identify five lead compounds: alfacalcidol (ALFA), chenodiol (CHEN), cyclophosphamide (CYCLO), fenbufen (FEN), and sulfaphenazole (SULFA). With the heat map visualization, we were able to identify several chemical classes present in our Prestwick library, in which all five compounds belong: vitamin D derivatives, steroids, cyclophosphamides, benzenes, and sulfonamides, respectively.

ALFA is known to be an active metabolite of vitamin D performing important functions in the regulation of calcium and bone metabolism [38]. Vitamin D hydroxylating enzymes and receptors are located on immune cells and in some key areas of the brain [39]. Epidemiological evidences demonstrated that deficiency of vitamin D is relevant to disease risk in multiple sclerosis (MS), Parkinson's disease (PD), and Alzheimer's disease (AD) [38, 40, 41]. Several studies done
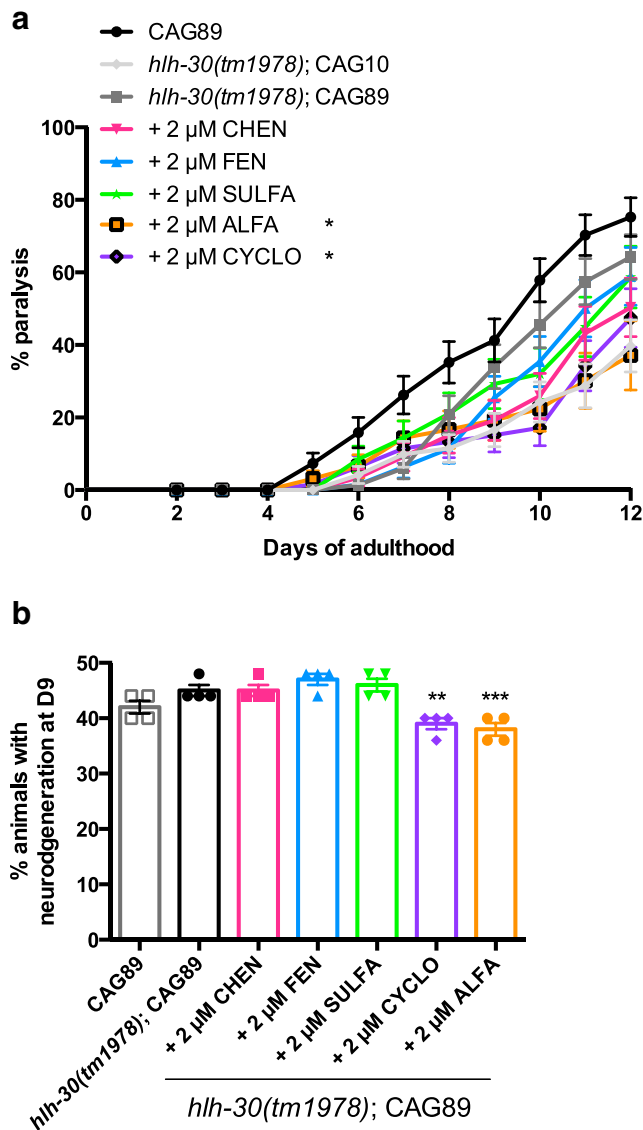
Fig. 6 CHEN, FEN, and SULFA require *hlh-30* for their neuroprotective activities. (**a**) *hlh-30(tm1978); ATXN3*-CAG89 worms showed a similar paralysis phenotype than the control, *ATXN3*-CAG89 mutants. When *hlh-30(tm1978); ATXN3*-CAG89 worms were treated with 2 μM CHEN, 2 μM FEN, or 2 μM SULFA, no rescue in the motility deficit was observed. Treatment with 2 μM CYCLO or 2 μM ALFA did rescue the motility defect (*$P < 0.05$ for each compound) (by log-rank (Mantel-Cox) test, $N = 90$–100 per trial, and $N = 270$–300 when all trials combined). These experiments were replicated 3 times. (**b**) Quantification of neurodegeneration in *hlh-30(tm1978)*; (*unc-47*p::mCherry; *ATXN3*-CAG89) worms at adulthood day nine. No rescue of neurodegeneration was observed in *hlh-30(tm1978)*; (*unc-47*p::mCherry; *ATXN3*-CAG89) worms at adulthood day nine when treated with 2 μM CHEN, 2 μM FEN, or 2 μM SULFA. Significant rescue of neurodegeneration in these worms when treated with 2 μM CYCLO (**$P < 0.01$) or 2 μM ALFA (***$P < 0.001$) (by one-way ANOVA test, $N = 100$ for each condition). These experiments were repeated 4 times

Fig. 7 Effect of the combination of the three *hlh-30* related compounds on MJD mutants. (**a**) No rescue of the locomotion impairment is observed in *hlh-30(tm1978); ATXN3*-CAG89 worms when treated with the three compounds simultaneously (by log-rank (Mantel-Cox) test, $N = 90$–100 per trial, and $N = 270$–300 when all trials combined). These experiments were replicated 3 times. (**b**) Significant rescue of the motility defect is observed in *hlh-30*::GFP; *ATXN3*-CAG89 worms when treated with the combination of the three compounds (**$P < 0.01$) (by log-rank (Mantel-Cox) test, $N = 270$–300). These experiments were repeated 3 times

on neurodegenerative diseases demonstrated that low serum or plasma vitamin D levels bring cognitive impairment, increased risk of dementia, and impaired motor functions [40,
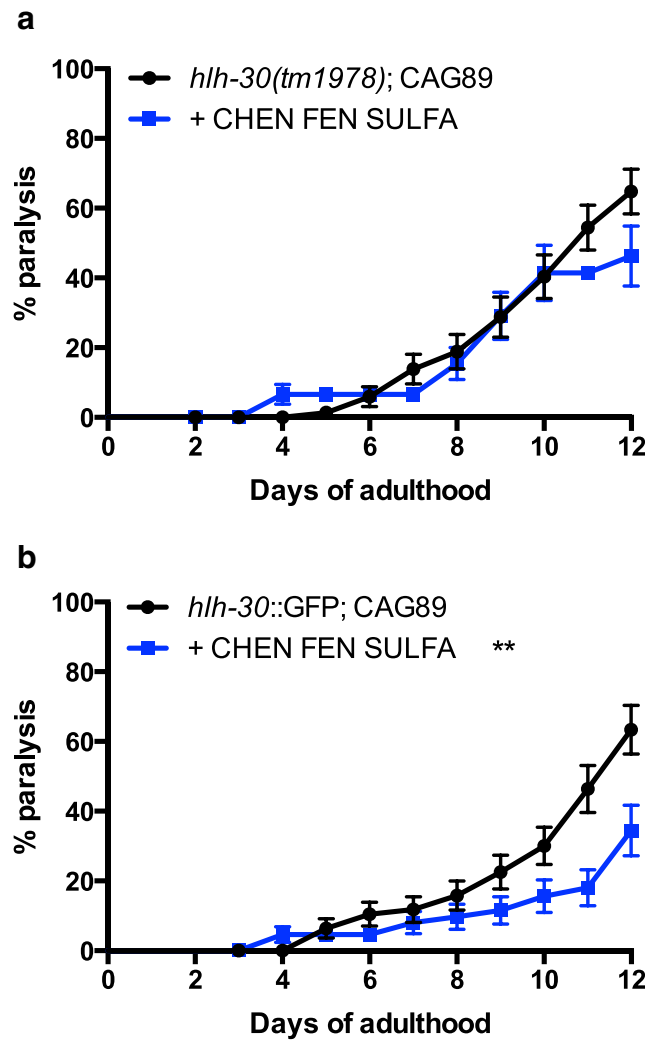
42–45]. Also, in a study evaluating the mechanisms by which vitamin D influences aging in *C. elegans*, it has been demonstrated that vitamin D promotes protein homeostasis, supresses protein insolubility and toxicity, and extends lifespan by specific stress response pathway genes [46]. Thus, these findings confirm the importance of keeping appropriate vitamin D serum levels and could explain the reason why many age-related diseases are related to vitamin D deficiency [46]. Moreover, a perturbation of calcium signaling in MJD cases has also been observed and as therapeutic perspectives, an improvement of the calcium homeostasis has been suggested [47]. Thereby, ALFA, being implicated in the

calcium hemostasis, might be one of the reasons why this compound figures among the leads. As an off-target effect, the use of vitamin D could also reverse the oxidative stress damage to DNA and protects against neuroinflammation [48, 49]. Treatment with alfacalcidol could decrease the neuronal toxicity caused by expanded ATXN3, which induces a high level of oxidative stress, DNA damage, disturbance in calcium signaling, and neuroinflammation in MJD patients [20, 47, 50, 51]. This compound could act on many different targets beneficial for MJD.

CHEN, also known as chenodeoxycholic acid, is a natural bile acid found in the body that dissolves the cholesterol that makes gallstones and inhibits its production in the liver and absorption in the intestine [52]. It has been noted that this compound displays also some off-target effects decreasing the neuronal toxicity. Indeed, it has been reported in a rat Alzheimer's disease model study that CHEN decreases the neurotoxicity and cognitive deterioration observed in this disease by activating the cAMP response element-binding protein (CREB), enhancing brain-derived neurotrophic factor (BDNF), and improving insulin sensitivity [52]. As for MJD, CHEN could be an interesting therapeutic approach to undertake in order to study these aspects as well. In this study, we showed a novel role for CHEN which figures among the leads. We have shown that CHEN requires *hlh-30,* a transcription factor related to the autophagy pathway, to complete its neuroprotective activities and decrease the neurotoxicity in our MJD model.

FEN is a non-steroidal anti-inflammatory drug predominantly used to treat inflammation. This compound prevents prostaglandin's production, which can cause inflammation by inhibiting cyclooxygenase (COX) [53]. FEN is used in Alzheimer's disease in order to prevent the inflammation observed in patients [54]. Several studies demonstrated the involvement of neuroinflammation in several neurodegenerative diseases such as Alzheimer's disease, Parkinson's disease, amyotrophic lateral sclerosis, Huntington's disease, and MJD [55–60]. Using FEN as a therapeutic compound could have clinical benefits such as decreasing the neuroinflammation in patients suffering from any of these neurodegenerative diseases. As an off-target effect, FEN also acts as an antioxidant. Indeed, this compound is able to scavenge reactive oxygen species (ROS) and reactive nitrate species (RNS) [61]. An interesting target to study in our MJD model in which we have already demonstrated high levels of oxidative stress [20]. In this study, we observed that FEN rescues phenotypes such as motility defects, neurodegeneration, and reduced longevity in *ATXN3*-CAG89 mutant worms. We also showed that FEN has high potential to rescue the motility deficit and neurodegeneration when TFEB/HLH-30 is overexpressed. This suggests that FEN could have beneficial and important effects on the autophagy pathway.

CYCLO, also known as cytophosphane, is an alkylating agent used in order to suppress the immune system, is an immunomodulator, and is also a potent anti-inflammatory [62]. This compound has been used as a preventative drug in multiple sclerosis disease. It has been shown that CYCLO has the property to permeate the blood-brain barrier, has a good bioavailability in the central nervous system, and, by exhorting its immunomodulation and immunosuppression role, is able to stabilize and prevent the progression of this disease [62, 63]. This drug is also used in individuals with mild to moderate Alzheimer's disease in order to decrease side effects [64]. This molecule is able to restore the motility deficit and neurodegeneration and enhance longevity in our MJD strain.

SULFA, finally, is a sulfonamide antibiotic that targets bacterial replication by inhibiting folate biosynthesis. It is also a selective inhibitor of the mammalian Cytochrome P450 isozyme CYP2C9 [65, 66]. This compound was also identified in a screen looking for molecules that block light-induced, degenerative loss of photoreceptors that occurs in age-related retinal degenerative diseases [67]. It has also been shown in a Parkinson's disease study that SULFA acts as a neuroprotective molecule by enhancing the longevity and normal dopaminergic neurons in their *C. elegans* model organism [66]. As an off-target effect, it has been shown that SULFA induces autophagy and protein kinase C (PKC) activations [68]. They have shown that the protection mediated by SULFA in their model was due to an increase in the autophagy process [68]. It has also been shown the autophagy activation is associated with neuroprotection [69]. As in this study, we showed that SULFA is dependent on *hlh-30,* an important regulator of the autophagy process, for its neuroprotective activities. We also showed that this compound is able to prolong longevity, as well as suppress neurodegeneration and motility defects in *ATXN3* worms.

Autophagy is one of the main and important pathways allowing the degradation of abnormal protein aggregates. Disruption and impairment of this pathway could contribute to many neurodegenerative diseases such as MJD [70–77]. It has also been shown that the upregulation of autophagy is capable of reducing the level of toxic proteins, ameliorate signs of disease, and also delay the disease progression in several neurodegenerative diseases such as Alzheimer's disease, Parkinson's diseases, polyglutamine diseases, and amyotrophic lateral sclerosis [32]. Based on these findings, we investigated if an important regulator of the autophagy process, TFEB/HLH-30, was involved in a model of MJD.

When TFEB/HLH-30 is overexpressed, we observed an increased level of *hlh-30*::GFP expression in our MJD mutants. Also, we observed a shift and increase of *hlh-30*::GFP expression during aging in our MJD mutants when treated with CHEN, FEN, and SULFA. In the early stages (adulthood days two and three), the compounds tend to decrease the level

of *hlh-30*::GFP expression in *ATXN3*-CAG89 worms perhaps as an early protective response in order to bring back the homeostasis. But then, at later stages (adulthood day five), with aging, they tend to increase the expression of *hlh-30*::GFP in our MJD mutants in order to protect and decrease the toxicity induced by mutant poly-Q proteins. Indeed, alterations of autophagy levels during aging have been reported and may be relevant to age-dependent neurodegeneration [78].

Also, it has been observed that the *hlh-30*::GFP reporter presents an increase in the level of fluorescence in the head (H), spermatheca (S), and tail (T) of adult animals. However, the reason explaining how this elevation could affect the GABAergic neurons (where *ATXN3* has been expressed in our transgenic MJD model) is due to the communication existing between cells during stress in order to augment coordination of an organism-wide stress response. Here, we suspect that proteotoxically stressed GABA neurons are communicating to the rest of the organism, something that we have previously reported for our MJD model in the context of ER stress [20].

ATXN3-CAG89 worms overexpressing TFEB/HLH-30 showed a rescue of motility deficits and neurodegeneration. Indeed, overexpression of this protein in our MJD model showed an ability to alleviate these phenotypes caused by the expanded ATXN3. A similar profile was observed when these worms were treated with small molecules. The lead compounds, CHEN, FEN, and SULFA rescued the locomotion defect and neurodegeneration in *ATXN3*-CAG89 worms overexpressing TFEB/HLH-30 when compared to *ATXN3*-CAG89 mutants. One compound, FEN, having an additive effect, showed high potential in decreasing remarkably the motor function and neurodegeneration (at adult day nine) in our mutant overexpressing TFEB/HLH-30 worms. Thus, a chemical-genetic approach could be a potential therapeutic strategy for MJD cases. These findings affirmed that TFEB/HLH-30 may be involved in ATXN3 phenotypes.

Finally, we demonstrated that CHEN, FEN, and SULFA require *hlh-30* for their neuroprotective activities. Indeed, these compounds are dependent and directly linked to this transcription factor to restore MJD phenotypes such as motility defect and neurodegeneration. In the absence of this gene, no small molecule mediated rescue is observed in our mutants. However, we observed that ALFA and CYCLO are still both able to rescue motility deficits as well as neurodegeneration in our MJD mutants. This rescue might be due to some compensatory effects of other activated pathways. Also, we observed a slight, non-significant decrease of paralysis phenotypes in our MJD model in the absence of *hlh-30*, suggesting a possible rescue effect. However, in the neurodegeneration assays, this rescue effect was completely absent, and we rather observed a slight increase (not significant) of neurodegeneration in the absence of *hlh-30* in *ATXN3*-CAG89 mutants. Based on

these observations, we concluded that the absence of *hlh-30* might not be toxic, as expected, in our MJD model, and shown to have a more neutral effect contrary to its overexpression, where we observed a significant decrease of paralysis and neurodegeneration phenotypes. This neutral effect observed in the LOF *hlh-30* might be due to a compensatory effect of other autophagy genes present in *C. elegans*.

In summary, we conducted a high-throughput screen of 3942 compounds using a *C. elegans* model of MJD. This screen led to the identification of five lead compounds that could be promising candidates for the treatment of MJD. Among the leads, one compound, fenbufen, showed to be the most effective. Indeed, additional studies are required to extend these findings to mammalian models of MJD. However, from a practical perspective, fenbufen, being FDA approved, could be a novel neuroprotective molecule to investigate since it could be translated rapidly into clinical settings for MJD.

Also, in this study, we identified TFEB/HLH-30 as a new potential regulator of MJD pathology. However, further investigation is required to better understand the roles of TFEB/HLH-30 and autophagy in the context of mutant *ATXN3* toxicity and MJD. Finally, the drug screening and the mutant *ATXN3* transgenic worms are valuable tools to advance MJD research, as the pathogenic mechanisms of disease are still not well understood. Our findings could guide future MJD research, by validating these lead molecules and autophagy regulators in more advanced model organisms and eventually in humans.

Compliance with Ethical Standards

Conflict of Interest The authors declare that they have no conflict of interest.

References

1. Schöls L, Bauer P, Schmidt T, Schulte T, Riess O. Autosomal dominant cerebellar ataxias: clinical features, genetics, and pathogenesis. Lancet Neurol 2004;35:291-304.

2. van de Warrenburg BP, Sinke RJ, Verschuuren-Bemelmans CC, et al. Spinocerebellar ataxias in the Netherlands: prevalence and age at onset variance analysis. Neurology 2002;585:702-8.

3. Da Silva JD, Teixeira-Castro A, Maciel P. From Pathogenesis to Novel Therapeutics for Spinocerebellar Ataxia Type 3: Evading Potholes on the Way to Translation. Neurotherapeutics 2019.

4. Xu Z, Tito AJ, Rui YN, Zhang S. Studying polyglutamine diseases in Drosophila. Exp Neurol 2015;274Pt A:25-41.

5. Matos CA, de Macedo-Ribeiro S, Carvalho AL. Polyglutamine diseases: the special case of ataxin-3 and Machado-Joseph disease. Prog Neurobiol 2011;951:26-48.

6. Teixeira-Castro A, Ailion M, Jalles A, et al. Neuron-specific proteotoxicity of mutant ataxin-3 in C. elegans: rescue by the DAF-16 and HSF-1 pathways. Hum Mol Genet 2011;2015:2996-3009.

7. Teixeira-Castro A, Jalles A, Esteves S, et al. Serotonergic signalling suppresses ataxin 3 aggregation and neurotoxicity in animal models of Machado-Joseph disease. Brain 2015;138Pt 11:3221-37.

8. Franca MC, Jr., D'Abreu A, Nucci A, Lopes-Cendes I. Muscle excitability abnormalities in Machado-Joseph disease. Arch Neurol 2008;654:525-9.

9. Bettencourt C, Santos C, Kay T, Vasconcelos J, Lima M. Analysis of segregation patterns in Machado-Joseph disease pedigrees. J Hum Genet 2008;5310:920-3.

10. Kawaguchi Y, Okamoto T, Taniwaki M, et al. CAG expansions in a novel gene for Machado-Joseph disease at chromosome 14q32.1. Nature genetics 1994;83:221-8.

11. Takiyama Y, Oyanagi S, Kawashima S, et al. A clinical and pathologic study of a large Japanese family with Machado-Joseph disease tightly linked to the DNA markers on chromosome 14q. Neurology 1994;447:1302-8.

12. Lima L, Coutinho P. Clinical criteria for diagnosis of Machado-Joseph disease: report of a non-Azorena Portuguese family. Neurology 1980;303:319-22.

13. Maciel P, Costa MC, Ferro A, et al. Improvement in the molecular diagnosis of Machado-Joseph disease. Archives of neurology 2001;5811:1821-7.

14. Cummings CJ, Zoghbi HY. Fourteen and counting: unraveling trinucleotide repeat diseases. Human molecular genetics 2000;96:909-16.

15. Wang G, Ide K, Nukina N, et al. Machado-Joseph disease gene product identified in lymphocytes and brain. Biochem Biophys Res Commun 1997;2332:476-9.

16. Shao J, Diamond MI. Polyglutamine diseases: emerging concepts in pathogenesis and therapy. Human molecular genetics 2007;16 Spec No. 2:R115-23.

17. Brenner S. The genetics of Caenorhabditis elegans. Genetics 1974;771:71-94.

18. Schmeisser K, Fardghassemi Y, Parker JA. A rapid chemical-genetic screen utilizing impaired movement phenotypes in C. elegans: Input into genetics of neurodevelopmental disorders. Exp Neurol 2017;293:101-14.

19. Stiernagle T. Maintenance of C. elegans. WormBook 2006:1-11.

20. Fardghassemi Y, Tauffenberger A, Gosselin S, Parker JA. Rescue of ATXN3 neuronal toxicity in Caenorhabditiselegans by chemical modification of endoplasmic reticulum stress. Dis Model Mech 2017;1012:1465-80.

21. Pohl F, Teixeira-Castro A, Costa MD, et al. GST-4-Dependent Suppression of Neurodegeneration in C. elegans Models of Parkinson's and Machado-Joseph Disease by Rapeseed Pomace Extract Supplementation. Front Neurosci 2019;13:1091.

22. Vaccaro A, Tauffenberger A, Aggad D, et al. Mutant TDP-43 and FUS cause age-dependent paralysis and neurodegeneration in C. elegans. PLoS One 2012;72:e31321.

23. Veriepe J, Fossouo L, Parker JA. Neurodegeneration in C. elegans models of ALS requires TIR-1/Sarm1 immune pathway activation in neurons. Nat Commun 2015;6:7319.

24. Cooper JF, Van Raamsdonk JM. Modeling Parkinson's Disease in C. elegans. J Parkinsons Dis 2018;81:17-32.

25. Alexander AG, Marfil V, Li C. Use of Caenorhabditis elegans as a model to study Alzheimer's disease and other neurodegenerative diseases. Front Genet 2014;5:279.

26. Griffin EF, Caldwell KA, Caldwell GA. Genetic and Pharmacological Discovery for Alzheimer's Disease Using Caenorhabditis elegans. ACS Chem Neurosci 2017;812:2596-606.

27. Patten SA, Parker JA, Wen XY, Drapeau P. Simple animal models for amyotrophic lateral sclerosis drug discovery. Expert Opin Drug Discov 2016;118:797-804.

28. Patten SA, Aggad D, Martinez J, et al. Neuroleptics as therapeutic compounds stabilizing neuromuscular transmission in amyotrophic lateral sclerosis. JCI Insight 2017;222.

29. Simonetta SH, Golombek DA. An automated tracking system for Caenorhabditis elegans locomotor behavior and circadian studies application. J Neurosci Methods 2007;1612:273-80.

30. Burns AR, Luciani GM, Musso G, et al. Caenorhabditis elegans is a useful model for anthelmintic discovery. Nat Commun 2015;6:7485.

31. Volpatti JR, Endo Y, Knox J, et al. Identification of drug modifiers for RYR1-related myopathy using a multi-species discovery pipeline. Elife 2020;9.

32. Djajadikerta A, Keshri S, Pavel M, et al. Autophagy Induction as a Therapeutic Strategy for Neurodegenerative Diseases. J Mol Biol 2019.

33. Lapierre LR, De Magalhaes Filho CD, McQuary PR, et al. The TFEB orthologue HLH-30 regulates autophagy and modulates longevity in Caenorhabditis elegans. Nat Commun 2013;4:2267.

34. Denzel MS, Lapierre LR, Mack HID. Emerging topics in C. elegans aging research: Transcriptional regulation, stress response and epigenetics. Mech Ageing Dev 2019;177:4-21.

35. Kwok TC, Ricker N, Fraser R, et al. A small-molecule screen in C. elegans yields a new calcium channel antagonist. Nature 2006;4417089:91-5.

36. O'Reilly LP, Luke CJ, Perlmutter DH, Silverman GA, Pak SC. C. elegans in high-throughput drug discovery. Adv Drug Deliv Rev 2014;69-70:247-53.

37. Ikenaka K, Tsukada Y, Giles AC, et al. A behavior-based drug screening system using a Caenorhabditis elegans model of motor neuron disease. Sci Rep 2019;91:10104.

38. Koduah P, Paul F, Dorr JM. Vitamin D in the prevention, prediction and treatment of neurodegenerative and neuroinflammatory diseases. EPMA J 2017;84:313-25.

39. Eyles DW, Smith S, Kinobe R, Hewison M, McGrath JJ. Distribution of the vitamin D receptor and 1 alpha-hydroxylase in human brain. J Chem Neuroanat 2005;291:21-30.

40. Balion C, Griffith LE, Strifler L, et al. Vitamin D, cognition, and dementia: a systematic review and meta-analysis. Neurology 2012;7913:1397-405.

41. Munger KL, Levin LI, Hollis BW, Howard NS, Ascherio A. Serum 25-hydroxyvitamin D levels and risk of multiple sclerosis. JAMA 2006;29623:2832-8.

42. Afzal S, Bojesen SE, Nordestgaard BG. Reduced 25-hydroxyvitamin D and risk of Alzheimer's disease and vascular dementia. Alzheimers Dement 2014;103:296-302.

43. Bischoff-Ferrari HA, Willett WC, Wong JB, et al. Fracture prevention with vitamin D supplementation: a meta-analysis of randomized controlled trials. JAMA 2005;29318:2257-64.

44. Peterson AL, Mancini M, Horak FB. The relationship between balance control and vitamin D in Parkinson's disease-a pilot study. Mov Disord 2013;288:1133-7.

45. Peterson AL, Murchison C, Zabetian C, et al. Memory, mood, and vitamin D in persons with Parkinson's disease. J Parkinsons Dis 2013;34:547-55.

46. Mark KA, Dumas KJ, Bhaumik D, et al. Vitamin D Promotes Protein Homeostasis and Longevity via the Stress Response Pathway Genes skn-1, ire-1, and xbp-1. Cell Rep 2016;175:1227-37.

47. Matos CA, de Almeida LP, Nobrega C. Machado-Joseph disease/spinocerebellar ataxia type 3: lessons from disease pathogenesis and clues into therapy. J Neurochem 2019;1481:8-28.

48. Haq SH, AlAfaleq NO, Johari RA. Vitamin D Treatment Reverses the Induced Oxidative Stress Damage to DNA. Pak J Biol Sci 2019;221:8-14.

49. Lima LAR, Lopes MJP, Costa RO, et al. Vitamin D protects dopaminergic neurons against neuroinflammation and oxidative stress in hemiparkinsonian rats. J Neuroinflammation 2018;151:249.

50. Chen YS, Hong ZX, Lin SZ, Harn HJ. Identifying Therapeutic Targets for Spinocerebellar Ataxia Type 3/Machado-Joseph Disease through Integration of Pathological Biomarkers and Therapeutic Strategies. Int J Mol Sci 2020;219.

51. Mendonca LS, Nobrega C, Tavino S, et al. Ibuprofen enhances synaptic function and neural progenitors proliferation markers and improves neuropathology and motor coordination in Machado-Joseph disease models. Hum Mol Genet 2019;2822:3691-703.

52. Bazzari FH, Abdallah DM, El-Abhar HS. Chenodeoxycholic Acid Ameliorates AlCl3-Induced Alzheimer's Disease Neurotoxicity and Cognitive Deterioration via Enhanced Insulin Signaling in Rats. Molecules 2019;2410.

53. Smith CE, Soti S, Jones TA, et al. Non-steroidal Anti-inflammatory Drugs Are Caspase Inhibitors. Cell Chem Biol 2017;243:281-92.

54. Walker D, Lue LF. Anti-inflammatory and immune therapy for Alzheimer's disease: current status and future directions. Curr Neuropharmacol 2007;54:232-43.

55. Harry GJ, Kraft AD. Neuroinflammation and microglia: considerations and approaches for neurotoxicity assessment. Expert Opin Drug Metab Toxicol 2008;410:1265-77.

56. Hirsch EC, Hunot S. Neuroinflammation in Parkinson's disease: a target for neuroprotection? Lancet Neurol 2009;84:382-97.

57. Hofmann KW, Schuh AF, Saute J, et al. Interleukin-6 serum levels in patients with Parkinson's disease. Neurochem Res 2009;348:1401-4.

58. van der Burg JM, Bjorkqvist M, Brundin P. Beyond the brain: widespread pathology in Huntington's disease. Lancet Neurol 2009;88:765-74.

59. Evert BO, Vogt IR, Kindermann C, et al. Inflammatory genes are upregulated in expanded ataxin-3-expressing cell lines and spinocerebellar ataxia type 3 brains. J Neurosci 2001;2115:5389-96.

60. Raposo M, Bettencourt C, Ramos A, et al. Promoter Variation and Expression Levels of Inflammatory Genes IL1A, IL1B, IL6 and TNF in Blood of Spinocerebellar Ataxia Type 3 (SCA3) Patients. Neuromolecular Med 2017;191:41-5.

61. Costa D, Moutinho L, Lima JL, Fernandes E. Antioxidant activity and inhibition of human neutrophil oxidative burst mediated by arylpropionic acid non-steroidal anti-inflammatory drugs. Biol Pharm Bull 2006;298:1659-70.

62. Duraes F, Pinto M, Sousa E. Old Drugs as New Treatments for Neurodegenerative Diseases. Pharmaceuticals (Basel) 2018;112.

63. Awad A, Stuve O. Cyclophosphamide in multiple sclerosis: scientific rationale, history and novel treatment paradigms. Ther Adv Neurol Disord 2009;26:50-61.

64. Aisen PS. The potential of anti-inflammatory drugs for the treatment of Alzheimer's disease. Lancet Neurol 2002;15:279-84.

65. Granville DJ, Tashakkor B, Takeuchi C, et al. Reduction of ischemia and reperfusion-induced myocardial damage by cytochrome P450 inhibitors. Proc Natl Acad Sci U S A 2004;1015:1321-6.

66. Wang S, Zhang S, Xu C, et al. Chemical Compensation of Mitochondrial Phospholipid Depletion in Yeast and Animal Models of Parkinson's Disease. PLoS One 2016;1110:e0164465.

67. Chang Q, Berdyshev E, Cao D, et al. Cytochrome P450 2C epoxygenases mediate photochemical stress-induced death of photoreceptors. J Biol Chem 2014;28912:8337-52.

68. Huang C, Liu W, Perry CN, et al. Autophagy and protein kinase C are required for cardioprotection by sulfaphenazole. Am J Physiol Heart Circ Physiol 2010;2982:H570-9.

69. Sheng R, Zhang LS, Han R, et al. Autophagy activation is associated with neuroprotection in a rat model of focal cerebral ischemic preconditioning. Autophagy 2010;64:482-94.

70. Nah J, Yuan J, Jung YK. Autophagy in neurodegenerative diseases: from mechanism to therapeutic approach. Mol Cells 2015;385:381-9.

71. Nixon RA. The role of autophagy in neurodegenerative disease. Nat Med 2013;198:983-97.

72. Fujikake N, Shin M, Shimizu S. Association Between Autophagy and Neurodegenerative Diseases. Front Neurosci 2018;12:255.

73. Sittler A, Muriel MP, Marinello M, et al. Deregulation of autophagy in postmortem brains of Machado-Joseph disease patients. Neuropathology 2018;382:113-24.

74. Onofre I, Mendonca N, Lopes S, et al. Fibroblasts of Machado Joseph Disease patients reveal autophagy impairment. Sci Rep 2016;6:28220.

75. Herzog LK, Kevei E, Marchante R, et al. The Machado-Joseph disease deubiquitylase ataxin-3 interacts with LC3C/GABARAP and promotes autophagy. Aging Cell 2020;191:e13051.

76. Duarte-Silva S, Silva-Fernandes A, Neves-Carvalho A, et al. Combined therapy with m-TOR-dependent and -independent autophagy inducers causes neurotoxicity in a mouse model of Machado-Joseph disease. Neuroscience 2016;313:162-73.

77. Watchon M, Yuan KC, Mackovski N, et al. Calpain Inhibition Is Protective in Machado-Joseph Disease Zebrafish Due to Induction of Autophagy. J Neurosci 2017;3732:7782-94.

78. Schmeisser K, Parker JA. Nicotinamide-N-methyltransferase controls behavior, neurodegeneration and lifespan by regulating neuronal autophagy. PLoS Genet 2018;149:e1007561.